Elementally Resolved Imaging of Dynamic Surface Processes: Chemical Waves in the System Rh(110)/NO + H_2

A. Schaak,[1] S. Günther,[2] F. Esch,[2] E. Schütz,[1] M. Hinz,[1] M. Marsi,[2] M. Kiskinova,[2] and R. Imbihl[1]
[1]*Institut für Physikalische Chemie und Elektrochemie, Universität Hannover, Callinstrasse 3-3a, D-30167 Hannover, Germany*
[2]*Sincrotrone Trieste, Area Science Park-Basovizza, I-34012 Trieste, Italy*
(Received 22 March 1999)

Chemically resolved *in situ* imaging of pulses in the system Rh(110)/NO + H_2 has been achieved with scanning photoelectron microscopy. Based on the experimental results a realistic mathematical model for the excitation of pulses was developed which reproduces the experimental concentration profiles.

PACS numbers: 82.65.Jv, 61.16.Ms, 82.20.Mj

An impressive variety of different chemical wave patterns has been found in recent years on catalytic single crystal surfaces but realistic mathematical models have so far been developed only for chemically very simple systems like catalytic CO oxidation on Pt surfaces [1–3]. The main obstacle in formulating realistic reaction-diffusion models for more complex reactions like NO + H_2 on Pt or Rh surfaces is the limited amount of information about the lateral distribution of adsorbate species on the surface. The main method for studying chemical wave patterns on surfaces has been photoelectron emission microscopy (PEEM) [3] which images primarily the work function and thus contains no or only very indirect information about the chemical identity of the adsorbate species.

In this paper we demonstrate that the potential of powerful synchrotron sources can be exploited to obtain chemically resolved *in situ* images of chemical waves. With the NO + H_2 reaction on Rh(110) we chose a relatively complex pattern forming system and we show that based on our measurements we can establish a realistic model for the formation of chemical waves in this system.

The NO + H_2 reaction on Rh(110) is an excitable medium, i.e., given sufficiently strong perturbation pulses ("chemical waves") are generated which travel across the surface forming typically target patterns and spiral waves [1]. While in a medium with isotropic diffusion the patterns are of concentric shape, rather unusual geometries of patterns were found in the NO + H_2 reaction on Rh(110): Rectangularly shaped target patterns and spiral waves and isolated traveling wave fragments have all been observed in this system [4–6]. The unusual types of patterns have been attributed to the presence of different N- and O-induced reconstructions with different diffusion anisotropies [5,7,8]. General activator-inhibitor models which have been modified to include the effect of state-dependent anisotropy were able to reproduce qualitatively all of the observed patterns [5]. No realistic model, however, has been formulated so far due to a lack of knowledge about the surface chemistry which is underlying these wave patterns.

In order to obtain concentration profiles of the relevant surface species for traveling pulses, *in situ* experiments with scanning photoelectron microscopy (SPEM) were performed at the electron storage ring ELETTRA. In SPEM photons (300–900 eV) from ELETTRA are focused into a 0.15 μm spot on the sample by means of a zone plate [9]. While the sample is rastered, photoelectrons are collected by a hemispherical energy analyzer (HE) tuned to the energy of a specific core level. In this way 2D maps of the surface composition with 0.15 μm spatial resolution are obtained. Wave patterns in the NO + H_2 reaction on Rh(110) were adjusted under isothermal conditions in the 10^{-7} mbar range operating the UHV chamber as a continuous flow reactor.

Under reaction conditions at $T \approx 500$ K NO dissociates readily on Rh(110) producing ordered overlayers of atomic oxygen and nitrogen which can be identified by their LEED patterns. In the pattern forming parameter range one observes a $c(2 \times 6)$-O for oxygen, a $(3 \times 1)/(2 \times 1)$-N for nitrogen, and, in addition, a $c(4 \times 2)$-2O,N representing a mixed overlayer [6,7,10–12]. Figure 1(a) displays a PEEM image of a target pattern in the NO + H_2 reaction on Rh(110). We can associate the dark areas indicative of a high work function with a predominantly oxygen covered surface ($\Delta\phi = 0.8$ eV) and the bright areas representing a low work function with an oxygen deficient surface, i.e., with a bare or nitrogen covered surface ($\Delta\phi = 0.3$ eV) [8]. Since conventional LEED (beam diameter ca. 0.5–1 mm) probes an area comparable to PEEM, a direct assignment of the different gray levels in Fig. 1(a) to various LEED structures is not possible [6].

At low $p\mathrm{H}_2$ and at high $p\mathrm{H}_2$ in PEEM a uniformly dark and a uniformly bright surface are present. Photoelectron spectra which were taken under these two limiting conditions are reproduced in Fig. 2. The spectra confirm that the increase in $p\mathrm{H}_2$ causes a complete removal of oxygen and induces a transformation into a nitrogen covered surface. The Rh 3*d* peak experiences a small shift of 0.1 eV to higher binding energy (BE) when the surface is oxygen covered. This allowed us to monitor the lateral variation in the chemical state of Rh by tuning to the lower or higher BE side of the peak during rastering.

Under the same reaction conditions under which the PEEM image in Fig. 1(a) was taken O1*s*, N1*s*, and

 0031-9007/99/83(9)/1882(4)$15.00

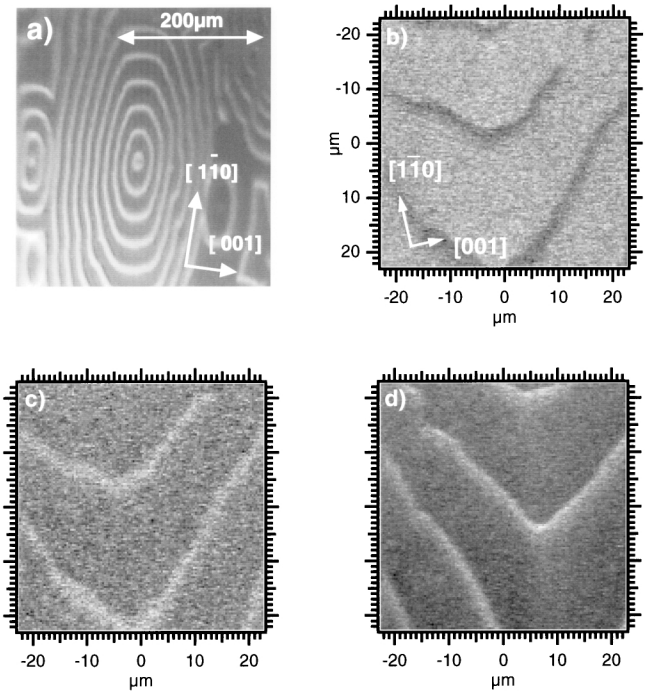

FIG. 1. Pulse propagation in the system Rh(110)/NO + H_2. (a) PEEM image of a target pattern. Experimental conditions: $T = 530$ K, $p_{NO} = 1.7 \times 10^{-7}$ mbar, $pH_2 = 7 \times 10^{-7}$ mbar. Elemental maps recorded with SPEM showing the distribution of the O1*s* (b) N1*s* (c) and Rh3$d_{5/2}$ (d) intensity during pulse propagation. The pulses propagate in the upward direction. Time per frame: 330 s; photon energy 625.7 eV. Experimental conditions: $T = 530$ K, $p_{NO} = 1.7 \times 10^{-7}$ mbar, $pH_2 = 6.4 \times 10^{-7}$ mbar.

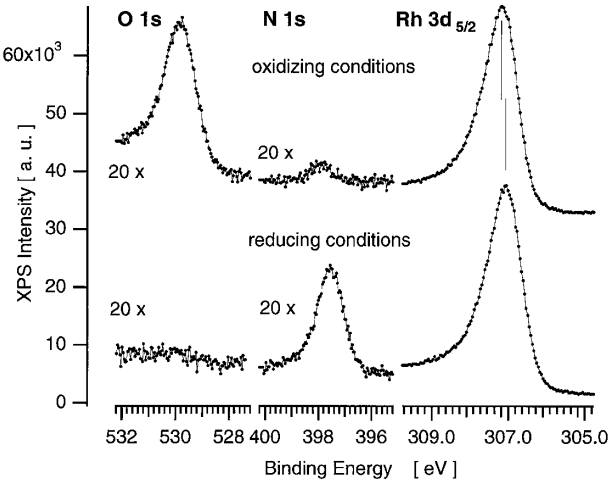

FIG. 2. Local (0.15 μm spot) photoelectron spectra of the Rh(110) surface under oxidizing ($p_{NO} = 1.5 \times 10^{-7}$ mbar, $pH_2 \approx 0$) and reducing conditions ($p_{NO} = 0.5 \times 10^{-7}$ mbar, $pH_2 = 1.2 \times 10^{-6}$) at $T = 530$ K. Photon energy = 625.7 eV. The residual intensity in the N1*s* region under oxidizing conditions is due to an Auger transition.

Rh3$d_{5/2}$ images of propagating pulses on Rh(110) were obtained as demonstrated by Figs. 1(b)–1(d). The pulses are roughly 5 μm wide and propagate with a velocity of 0.5 μm/s. The contrast in the Rh images reflects the shift of the Rh peak out of the energy window of the HE which was centered to the low BE side of the Rh peak. In order to be able to correlate the different elemental maps a pulse moving perpendicular to the scan direction was selected, and while a 2D scan was performed the analyzer energy was rapidly switched between the different binding energies. From the x-ray photoelectron spectroscopy (XPS) intensities absolute coverages were obtained by calibrating the XPS peaks in Fig. 2 with LEED structures of known coverages, i.e., a $c(2 \times 6)$-O with $\theta_O = 0.66$ and a (2×1)-N with $\theta_N = 0.5$ [7].

The resulting concentration profile in Fig. 3(a) reveals that in each pulse the $c(2 \times 6)$-O high oxygen coverage phase is practically completely reacted away and replaced by a nitrogen adlayer which reaches the ideal coverage $\theta_N = 0.5$ associated with the (2×1)-N. In the refractory tail oxygen and nitrogen are coadsorbed over a wide range which can be assigned to the $c(4 \times 2)$-2O,N structure as confirmed by independent experiments [13].

Neglecting the very small amount of NH_3 and N_2O production at low p and OH and NH_x intermediates we can formulate the reaction steps as follows:

$$H_2 + 2^* \leftrightarrow 2H_{ad}\,, \tag{R1}$$

$$NO + * \leftrightarrow NO_{ad}\,, \tag{R2}$$

$$NO_{ad} + * \rightarrow N_{ad} + O_{ad}\,, \tag{R3}$$

$$2N_{ad} \rightarrow N_2 + 2^*, \tag{R4}$$

$$O_{ad} + 2H_{ad} \rightarrow H_2O + 3^*, \tag{R5}$$

where * denotes a vacant adsorption site.

Pulses very similar to Rh(110) but isotropic have also been observed in the NO + H_2 reaction on Rh(111) [14,15]. Rh(111) is structurally very stable, and we therefore conclude that structural transformation of the substrate cannot be essential for the excitation mechanism. For a mathematical model we accordingly neglect structural changes of the substrate and consider only the reaction steps R1–R5 resulting in a set of differential equations for the coverage of hydrogen (θ_H), NO (θ_{NO}), nitrogen (θ_N), and oxygen (θ_O):

$$\begin{aligned}\frac{\partial\theta_H}{\partial t} &= k_1 p_{H_2}(1 - \theta_H - \theta_{NO} - \alpha\theta_N - \beta\theta_O)^2 \\ &\quad + \gamma k_1 p_{H_2}(1 - \theta_H)^2 \\ &\quad - k_2\theta_H^2 - 2k_3\theta_O\theta_H + \nabla\cdot[D_H(1 - \delta\theta_N)\nabla\theta_H],\end{aligned}$$

$$\begin{aligned}\frac{\partial\theta_{NO}}{\partial t} &= k_4 p_{NO}(1 - \theta_H - \theta_{NO} - \theta_O) - k_5\theta_{NO} \\ &\quad - k_6\theta_{NO}(1 - \theta_{NO} - \theta_O),\end{aligned}$$

$$\frac{\partial\theta_N}{\partial t} = k_6\theta_{NO}(1 - \theta_{NO} - \theta_O) - k_7\theta_N^2\,,$$

$$\frac{\partial\theta_O}{\partial t} = k_6\theta_{NO}(1 - \theta_{NO} - \theta_O) - k_3\theta_O\theta_H\,.$$

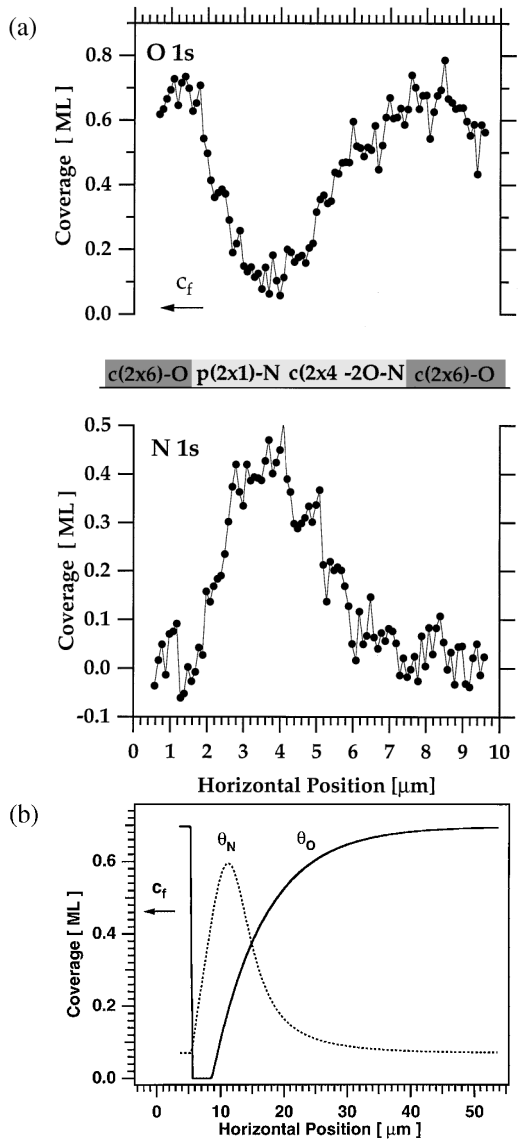

FIG. 3. Comparison of experimentally determined and simulated concentration profile for a propagating pulse. (a) Experimental profile. Conditions as in Fig. 1(a). The panel at the bottom indicates the corresponding sequence of LEED structures [13]. (b) Simulation of a pulse using the mathematical model described in the text. Parameters: $T = 530$ K, $p_{NO} = 2.0 \times 10^{-7}$ mbar, $pH_2 = 6.0 \times 10^{-7}$ mbar; prefactors $\alpha = 2.0$, $\beta = 2.0$, $\gamma = 0.017$, $\delta = 4.0$; $E_{rep} = 32$ kJ/mol.

The model contains the adsorption (k_1, k_4) and desorption (k_2, k_5) of the two reacting gases, the dissociation of NO (k_6), the associative desorption of adsorbed nitrogen (k_7), water formation (k_3), and the surface diffusion of atomic hydrogen (D_H). Compared to the very mobile hydrogen all other adsorbates diffuse slowly. The expressions in parentheses describe site blocking effects. In order to account for different inhibitory effects of the adsorbates we use prefactors denoted here with greek letters (α, β, δ). In the simulations all terms in parentheses are set equal to zero when they become negative. For simplicity, saturation coverages of one have been assumed for oxygen and nitrogen but since N_{ad} and O_{ad} occupy different sites the total coverage may exceed one [7,12].

To account for the experimental observation that even a fully oxygen covered surface cannot completely inhibit hydrogen adsorption, we introduce surface defects in the term with γ. Experimentally it has been shown that on a well-prepared (2×1)-N adlayer NO can still adsorb and dissociate and, accordingly, in the model N_{ad} does not inhibit NO dissociation (k_6 term) [8]. We also introduce a simple site blocking factor δ of atomic nitrogen for the diffusion of atomic hydrogen because in a similar system, $Rh(111)/NO + H_2$, atomic nitrogen acts as a diffusion barrier for hydrogen thus restricting the long range interaction of pulses [14]. The constants $k_1 - k_7$ and D_H were taken from experimental data as summarized in Table I; the prefactors α, etc., were obtained by fitting to experimental data.

A drastic effect which turned out to be crucial for the excitation mechanism is the strong repulsive interaction between atomic oxygen and nitrogen as evidenced in thermal desorption (TD) spectroscopy by a downward shift by $\approx$100 K of the N_2 desorption peak maximum when nitrogen is coadsorbed with oxygen [11]. In the model we assume a linear decrease of the activation energy, E_7, for N_2 desorption with oxygen coverage, i.e., $E_7 = E_7^0 - \theta_O E_{rep}$, and fit E_{rep} to experimental TD data [8,11]. The numerical integration of the above model yields traveling pulse solutions shown in Fig. 3(b) with a pulse velocity $c_f = 0.3$ μm/s similar to the experiment. The excitation mechanism for a pulse can be described by the following sequence of steps.

(i) Starting with a completely oxygen covered surface hydrogen can adsorb only at some defect. Adsorbed oxygen is reactively removed by hydrogen and a reaction front spreads out.

(ii) On the largely adsorbate free surface thus created hydrogen and NO can adsorb and dissociate uninhibitedly. Since oxygen is removed through reaction with hydrogen, nitrogen accumulates.

TABLE I. Constants used in the simulation. The T dependence of the constants is described by an Arrhenius expression $k_i = \nu_i \exp(E_i/RT)$.

Constant k_i	ν_i	E_i[kJ/mol]	Ref.
	2.186×10^6		
k_1	ML s^{-1} $mbar^{-1}$	...	[16]
k_2	3×10^{10} s^{-1}	75	[17]
k_3	1×10^{13} s^{-1}	84	[18]
	0.189×10^6		
k_4	ML s^{-1} $mbar^{-1}$	...	[19]
k_5	1×10^{13} s^{-1}	126	[19] + fit
k_6	1×10^{7} s^{-1}	45	[20]
k_7	1×10^{10} s^{-1}	118	[11] + fit
D_H	3.8×10^{-3} cm^2 s^{-1}	45	[21]

(iii) On the nitrogen covered surface NO can still adsorb and dissociate. The oxygen coverage thus increases leading through repulsive interactions to the destabilization of nitrogen which desorbs. The initial state of an oxygen covered surface is finally restored.

The key element in the excitation mechanism is given by a well established fact, the destabilization of chemisorbed nitrogen by coadsorbed oxygen [11]. A comparison of different Rh orientations reveals that, in fact, only those surfaces in the $NO + H_2$ reaction display oscillatory/excitable behavior where nitrogen is not bonded too strongly [22].

In summary, we have shown that elementally resolved imaging of chemical waves with SPEM is an important tool to understand the chemistry and the dynamics of complex surface reactions. This was demonstrated here with the chemical waves in the system $Rh(110)/NO + H_2$ for which a realistic mathematical model was developed which contains no arbitrary assumptions and semiquantitatively reproduces the experimental results.

We thank Diego Lonza and Dr. M. Gentile (IESS). This work was financially supported by EC grant under Contract No. EBRCH-GECT920013 and Sincrotrone Trieste SCpA.

[1] M. Eiswirth and G. Ertl, in *Chemical Waves and Patterns*, edited by R. Kapral and K. Showalter (Kluwer, Dordrecht, 1994).
[2] R. Imbihl and G. Ertl, Chem. Rev. **95**, 697 (1995).
[3] H. H. Rotermund, Surf. Sci. Rep. **29**, 265 (1997).
[4] F. Mertens and R. Imbihl, Nature (London) **370**, 124 (1994).
[5] N. Gottschalk, F. Mertens, M. Bär, M. Eiswirth, and R. Imbihl, Phys. Rev. Lett. **73**, 3483 (1994).
[6] F. Mertens and R. Imbihl, Surf. Sci. **347**, 355 (1996).
[7] M. Kiskinova, Chem. Rev. **96**, 1431 (1996).
[8] F. Mertens, S. Schwegmann, and R. Imbihl, J. Chem. Phys. **106**, 4319 (1997).
[9] M. Marsi, L. Casalis, L. Gregoratti, S. Günther, A. Kolmakov, J. Kovac, D. Lonza, and M. Kiskinova, J. Electron Spectrosc. Relat. Phenom. **84**, 73 (1997).
[10] G. Comelli, V. R. Dhanak, M. Kiskinova, K. C. Prince, and R. Rosei, Surf. Sci. Rep. **32**, 165 (1998).
[11] M. Kiskinova, S. Lizzit, G. Comelli, G. Paolucci, and R. Rosei, Appl. Surf. Sci. **64**, 185 (1993).
[12] M. Gierer, F. Mertens, H. Over, G. Ertl, and R. Imbihl, Surf. Sci. **339**, L903 (1995).
[13] A. Schaak *et al.* (to be published).
[14] N. M. H. Janssen, A. Schaak, B. E. Nieuwenhuys, and R. Imbihl, Surf. Sci. **364**, L555 (1996).
[15] A. G. Makeev *et al.*, J. Chem. Phys. **105**, 7210 (1996); **107**, 965 (1997).
[16] M. Ehsasi and K. Christmann, Surf. Sci. **194**, 172 (1988).
[17] A. Baraldi, V. R. Dhanak, G. Comelli, K. C. Prince, and R. Rosei, Surf. Sci. **293**, 246 (1993).
[18] M. L. Wagner and L. D. Schmidt, J. Phys. Chem. **99**, 805 (1995).
[19] M. Bowker, Q. Guo, and R. W. Joyner, Surf. Sci. **257**, 33 (1991).
[20] H. J. Borg, J. F. C.-J. M. Reijerse, R. A. van Santen, and J. W. Niemandsverdriet, J. Chem. Phys. **101**, 10 052 (1994).
[21] A. Schaak, S. Shaikhutdinov, and R. Imbihl, Surf. Sci. **421**, 191 (1999).
[22] N. M. H. Janssen, B. E. Nieuwenhuys, M. Ikai, K. Tanaka, and A. R. Cholach, Surf. Sci. **319**, L29 (1994).